

Supporting Information for: Performance Enhancement of Polymer-Based Solar Cells by Induced Phase-Separation with Silica Particles

Hao Shen, Néstor E. Valadez-Pérez, Brett Guralnick, Yun Liu, and Michael E. Mackay

1 X-ray photoelectron spectroscopy

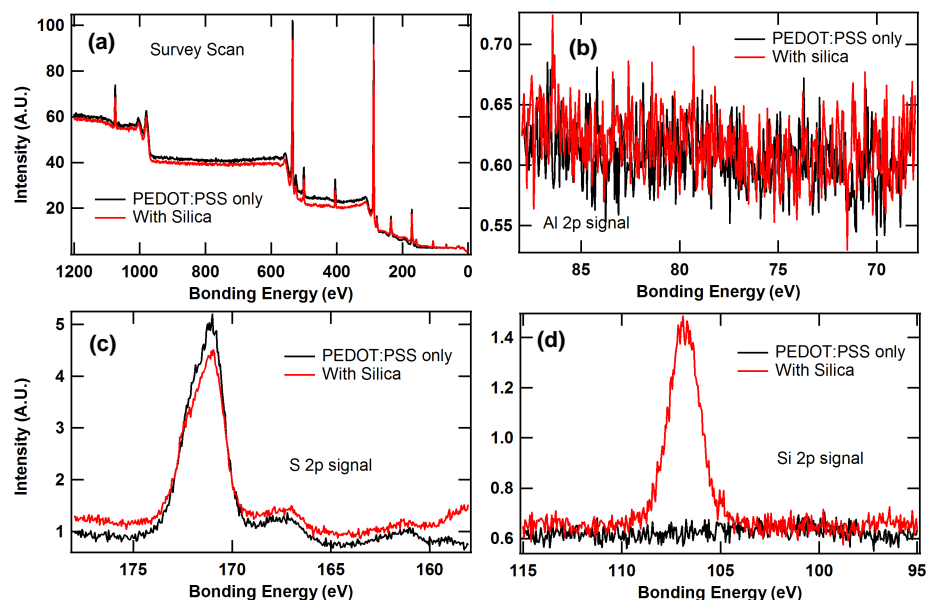


Figure S1 XPS data of the PEDOT:PSS coated sapphire substrate. (a) Survey scan (b) Al 2p (c) S 2p (d) Si 2p.

In order to ensure the silica-PEDOT:PSS layer coated the entire substrate, x-ray photoelectron spectroscopy (XPS) was used to probe the atomic composition on the surface, as shown in Fig. S1. Sapphire substrates were used in this experiment to distinguish between the signal from the substrate and the top layer containing PEDOT:PSS and silica. Figure S1 (b) shows the Al 2p signal from the samples coated with PEDOT:PSS with or without silica particles. The absence of the Al 2p peak

is the evidence of complete coverage of the substrate in both cases. The panel (c) shows the S 2p peaks. We found the sulfur signal coming from the surface of PEDOT:PSS is reduced due to the occupation of silica on the substrate. Shown in panel (d) is the Si 2p signal. As expected, only samples with silica show signals at this energy level. From the XPS results, we conclude the PEDOT:PSS coated the entire substrate surface with or without silica particles. However, the PEDOT:PSS did not completely cover the top of the particle, leaving the surface of silica exposed to the detector. Therefore, we expect those silica surfaces would contact with the subsequently coated active layer.

2 Schulz size distribution of spheres

Schulz size distribution is used for many poly-dispersed polymer and colloidal systems. This two-parameter probability distribution function for radii of the spheres is written as:

$$f(R) = (z+1)^{z+1} \left(\frac{R}{R_{avg}}\right)^z \frac{\exp[-(z+1)\frac{R}{R_{avg}}]}{\Gamma(z+1)R_{avg}} \quad (S1)$$

where R_{avg} is the number-averaged (arithmetic mean) radius and z is related to polydispersity, p , by:

$$z = \frac{1}{p^2} - 1 \quad (S2)$$

$$p = \frac{\sigma}{R_{avg}} \quad (S3)$$

where σ is variance of the distribution.

In a scattering experiment, the scattering intensity is often normalized to the volume of the scatters. The average volume of spheres following Schulz distribution is given as:

$$\langle V \rangle = \frac{4\pi}{3} \langle R^3 \rangle = \frac{4\pi}{3} R_{avg}^3 \frac{(z+3)(z+2)}{(z+1)^2} \quad (S4)$$

where $\langle R^3 \rangle$ is the volume-averaged radius.

The scattering intensity from Schulz spheres is:

$$I(q) = \frac{\phi(\Delta\rho)^2}{\langle V \rangle} \int f(R) \left(\frac{4\pi R^3}{3}\right)^2 \frac{9[\sin(qR) - qR\cos(qR)]^2}{(qR)^6} dR \quad (S5)$$

Table S1 lists sizes of the silica particles measured by SANS as dilute colloids or coated on silicon wafers with PEDOT:PSS.

Table S1 Sizes of silica nanoparticles from SANS data fitted with Schulz sphere model

Quantity	Unit	Dilute colloids	Coated on silicon wafers with PEDOT:PSS
Volume fraction ϕ	-	0.00591	0.0418
Polydispersity p	-	0.166	0.142
z	-	35.2	48.6
R_{avg}	nm	62.9	65.8
$\langle R^3 \rangle$	nm	68.1	69.8

3 Guinier analysis on the silica particles

Guinier plots were used to obtain the radii of gyration (R_g) of the silica particles as dilute colloids or coated. The SANS data is plotted as $\ln(I)$ vs. q^2 . In the linear region of the data at small q (Guinier approximation), the R_g can be obtained by fitting the data to the following equation:

$$\ln(I) = \ln(I_0) - \frac{q^2 R_g^3}{3} \quad (\text{S6})$$

Notice that $qR_g < \sqrt{3}$ to use this approximation. The radius of a sphere can also be obtained by $\sqrt{\frac{5}{3}}R_g$.

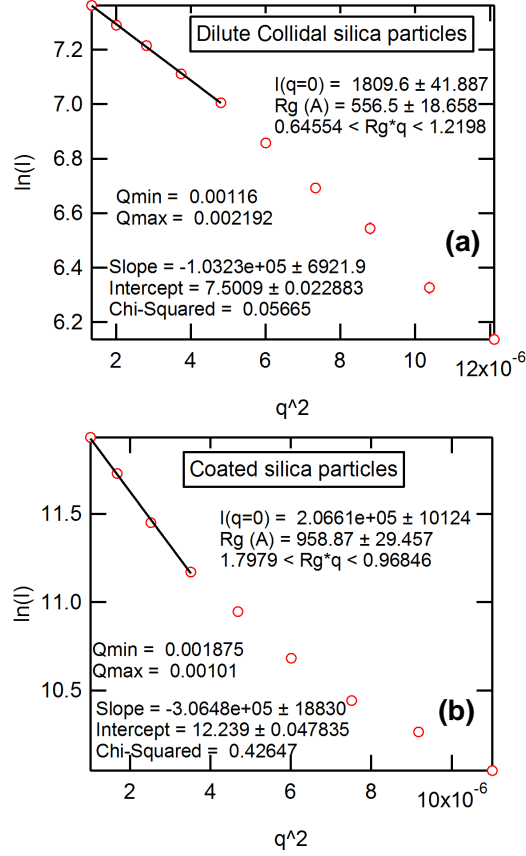


Figure S2 Guinier plots of silica particles as (a) Dilute colloids. (b) Coated on the silica wafers with PEDOT:PSS.

4 Teubner-Strey model and the original fitting parameters

In some conventions, the Teubner-Strey function is written in the following form:

$$I(q) = \frac{1}{a'_2 + c'_1 q^2 + c'_2 q^4} + bkg \quad (S7)$$

instead of its original version¹ described in the main text:

$$I(q) = \frac{\phi_p(\Delta\rho)^2 \left(\frac{8\pi}{\xi}\right)}{\frac{a_2}{c_2} + \frac{c_1}{c_2}q^2 + q^4} + bkg \quad (\text{S8})$$

However, the equations for deriving d (Eqn. 2) and ξ (Eqn. 3) are the same if a_2 , c_1 and c_2 are substituted with a'_2 , c'_1 and c'_2 , respectively. The only difference between these two conventions is how the scaling of the equation is incorporated into c'_2 . Comparing Eqns. S7 and S8, one can find:

$$\frac{1}{c'_2} = \phi_p(\Delta\rho)^2 \left(\frac{8\pi}{\xi}\right) \quad (\text{S9})$$

or

$$\phi_p(\Delta\rho)^2 = \left(\frac{\xi}{8\pi c'_2}\right) = SF \quad (\text{S10})$$

Here we provide the original Teubner-Strey fitting parameters in the form of Eqn. S7.

Also, The combined model of Schulz spheres and Teubner-Strey used for the SANS data with silica particles is written as:

$$I(q) = \frac{1}{a'_2 + c'_1 q^2 + c'_2 q^4} + \frac{\phi(\Delta\rho)^2}{\langle V \rangle} \int f(R) \left(\frac{4\pi R^3}{3}\right)^2 \frac{9[\sin(qR) - qR \cos(qR)]^2}{(qR)^6} dR + bkg \quad (\text{S11})$$

Tables S2 and S3 list the original fitting parameters for all the SANS data of P3HT:PCBM active layers.

Table S2 Original fitting parameters for samples without the silica particles.

Parameter	Unit	PCBM weight %, As-Cast				
		10 %	20 %	30 %	40 %	50 %
a'_2	10^{-2} cm	8.13	2.31	1.53	1.77	0.540
c'_1	10^1 cmÅ ²	-7.03	-3.40	-2.38	-2.37	-0.557
c'_2	10^4 cmÅ ⁴	9.63	4.45	3.03	3.21	1.89
bkg	10^{-1} cm ⁻¹	5.18	3.54	3.07	5.38	3.74
d	Å	248	267	267	267	340
ξ	Å	60.1	76.9	79.4	73.2	71.9
SF	10^{-12} Å ⁻⁴	0.248	0.688	1.04	0.907	1.51

Parameter	Unit	PCBM weight %, Annealed				
		10 %	20 %	30 %	40 %	50 %
a'_2	10^{-2} cm	15.7	4.01	1.86	0.870	0.399
c'_1	10^1 cmÅ ²	-16.4	-6.47	-3.55	-1.64	-0.854
c'_2	10^4 cmÅ ⁴	12.7	5.69	3.21	1.98	1.79
bkg	10^{-1} cm ⁻¹	5.19	3.50	2.81	4.61	3.56
d	Å	212	237	245	270	333
ξ	Å	65.4	86.0	98.0	89.9	92.5
SF	10^{-12} Å ⁻⁴	0.205	0.601	1.21	1.81	2.06

Note: a'_2 , c'_1 , c'_2 and bkg are obtained from the fitting results with Eqn. S7. d , ξ and SF are calculated according to Eqns. 2, 3, and S10.

Table S3 Original fitting parameters for samples with the silica particles.

Parameter	Unit	PCBM weight %, As-Cast				
		10 %	20 %	30 %	40 %	50 %
R_{avg}	Å	435	292	243	220	263
p	-	0.301	0.330	0.330	0.330	0.254
$\Delta\rho$	10^{-6}Å^{-2}	2.68	2.68	2.68	2.68	2.68
ϕ	10^{-2}	1.09	1.02	1.36	3.60	3.79
a'_2	10^{-2}cm	6.08	0.908	0.653	0.445	0.285
c'_1	10^1cmÅ^2	-2.01	-0.878	-1.30	-0.911	-0.674
c'_2	10^4cmÅ^4	8.07	2.75	2.60	2.34	2.15
bkg	10^{-1}cm^{-1}	4.62	9.27	5.02	4.93	7.68
d	Å	282	328	324	354	389
ξ	Å	51.9	69.4	89.4	91.1	98.2
SF	10^{-12}Å^{-4}	0.256	1.01	1.37	1.55	1.82

Parameter	Unit	PCBM weight %, Annealed				
		10 %	20 %	30 %	40 %	50 %
R_{avg}	Å	421	352	242	199	193
p	-	0.362	0.330	0.330	0.330	0.254
$\Delta\rho$	10^{-6}Å^{-2}	2.68	2.68	2.68	2.68	2.68
ϕ	10^{-2}	1.29	0.906	1.44	2.95	6.06
a'_2	10^{-2}cm	13.3	1.38	0.897	0.596	0.352
c'_1	10^1cmÅ^2	-8.88	-1.23	-1.79	-1.58	-0.869
c'_2	10^4cmÅ^4	9.52	3.57	3.42	3.08	2.42
bkg	10^{-1}cm^{-1}	5.21	10.4	6.16	6.52	8.61
d	Å	219	315	319	337	375
ξ	Å	52.9	66.6	89.4	104	99.6
SF	10^{-12}Å^{-4}	0.221	0.743	1.04	1.35	1.64

Note: R_{avg} , p , ϕ , a'_2 , c'_1 , c'_2 and bkg are obtained from the fitting results with Eqn. S11. $\Delta\rho$ is an arbitrary number because the contrast between the silica-PCBM to the matrix is unknown. d , ξ and SF are calculated according to Eqns. 2, 3, and S10.

5 Equations for mass conservation and scale factor

For the equation of PCBM mass conservation, assuming the volume of PCBM and P3HT is additive, the weight fraction of PCBM in the solid of the cast solution can be converted to the overall bulk volume fraction

of PCBM:

$$\phi^* = \frac{\frac{w^*}{\rho_{PCBM}^*}}{\frac{w^*}{\rho_{PCBM}^*} + \frac{1-w^*}{\rho_{P3HT}^*}} \quad (\text{S12})$$

where

ϕ^* : Overall bulk volume fraction of PCBM, with respect to the volume of the BHJ film

w^* : Weight fraction of PCBM in the solid of the cast solution

ρ_{PCBM}^* : Density of PCBM,² 1.3 g/cm³

ρ_{P3HT}^* : Density of P3HT,² 1.15 g/cm³

Then, mass conservation of PCBM from the cast solution can be written as:

$$\phi^* = \phi_p + \phi_m \quad (\text{S13})$$

where

ϕ_p : Volume fraction of phase-separated PCBM observed in SANS, with respect to the volume of the BHJ film

ϕ_m : Volume fraction of PCBM dissolved in the matrix, with respect to the volume of the BHJ film

Notice the volume fraction here is based on the total volume of the BHJ. When we discuss the miscibility of PCBM in the matrix, we want the fraction of PCBM in the *volume of the matrix*. Therefore, we slightly change the notation of ϕ_m to define ϕ_m' , which is the volume fraction of PCBM dissolved in the matrix, with respect to the volume of the matrix. In our two-phase model, the matrix is the space in the BHJ active layer not occupied by the phase-separated PCBM, ϕ_p . Therefore the conversion between ϕ_m and ϕ_m' is:

$$\phi_m' = \frac{\phi_m}{1 - \phi_p} \quad (\text{S14})$$

The denominator means the volume in the BHJ layer excluded by the PCBM phase, which is the volume of the matrix. Combining Eqn. S13 and Eqn. S14, we have

$$\phi^* = \phi_m'(1 - \phi_p) + \phi_p \quad (\text{S15})$$

This is the mass balance equation of the system. The subtle difference in the definitions between ϕ_m and ϕ_m' causes the non-linearity of the mass conservation contour curves on Fig. 8 in the main text.

For the equation of the scale factor, considering the SLD of the matrix as a function of ϕ_m' :

$$\rho_{matrix} = \phi_m' \rho_{PCBM} + (1 - \phi_m') \rho_{P3HT} \quad (S16)$$

where

ρ_{matrix} : SLD of the matrix (mixture of P3HT and PCBM)

ρ_{PCBM} : SLD of PCBM

ρ_{P3HT} : SLD of P3HT

The contrast term in the system, $\Delta\rho$, is defined as $(\rho_{PCBM} - \rho_{matrix})$. With Eqn. S16 and some simplification, we can rewrite it as:

$$\Delta\rho = (1 - \phi_m')(\rho_{PCBM} - \rho_{P3HT}) \quad (S17)$$

Since ρ_{PCBM} and ρ_{P3HT} are known constants, $\Delta\rho$ is a linear transformation of ϕ_m' . Therefore, SF can be expressed as $\phi(\Delta\rho)^2$, a function of $(\phi, \Delta\rho)$, or a function of (ϕ, ϕ_m') by using Eqn. S17. We choose the latter form because ϕ_m' indicates the solubility of PCBM in the matrix, a more relevant physical quantity to our interests. Hence,

$$SF = \phi_p(1 - \phi_m')^2(\rho_{PCBM} - \rho_{P3HT})^2 \quad (S18)$$

Now that the mass conservation and scale factor are both explicit functions of ϕ and ϕ_m' , Fig. 8 can be constructed accordingly.

6 Grazing incident x-ray diffraction (GIXRD)

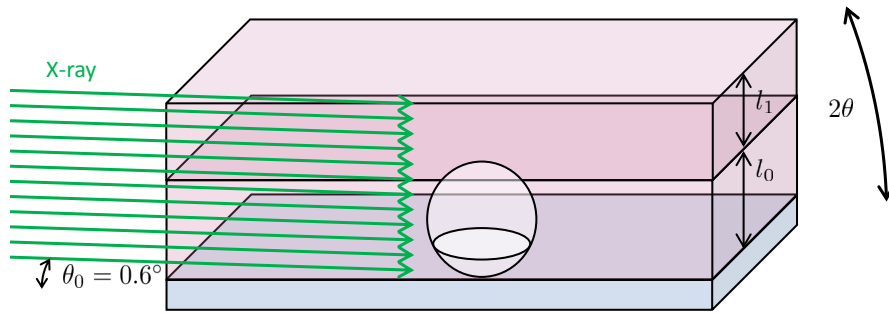


Figure S3 Geometry of the GIXRD setup.

Grazing incident x-ray diffraction (GIXRD) was done with a Rigaku Ultima IV diffractometer by using $\text{CuK}\alpha$ radiation at a fixed incident

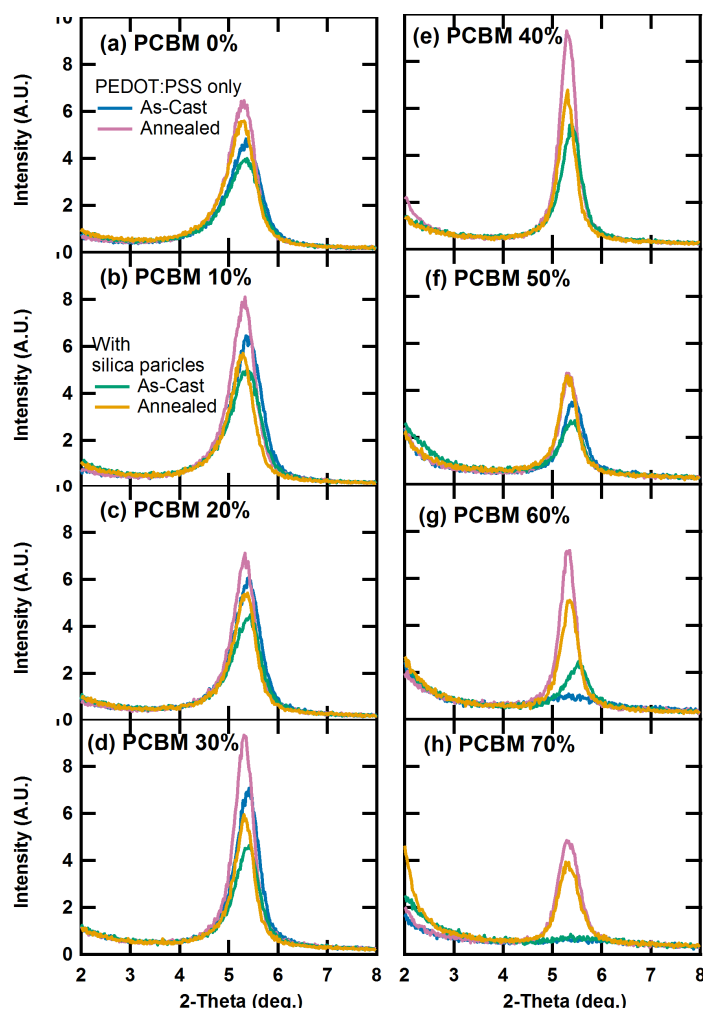


Figure S4 GIXRD results of P3HT:PCBM active layers.

angle of 0.6 degree. The receiving side was a pencil detector directly facing the incident x-ray beam moving in $2-\theta$ direction. The geometry of the setup is schematically shown in Fig. S3.

The samples were prepared using the same protocol described in the experimental section on the silica wafers coated PEDOT:PSS with or without the silica particles. Each set of as-cast and annealed data was from the same sample before and after annealing. The data is shown in Fig. S4.

We found out the inclusion of silica particles reduced the intensity of

the signal due to the attenuation effect. The attenuation of x-rays can be described by the following equation:

$$\frac{I}{I_0} = \exp \left[-\left(\frac{\mu}{\rho}\right)x \right] \quad (\text{S19})$$

where $\left(\frac{\mu}{\rho}\right)$ is the mass attenuation coefficient, ρ the density of the material, and x the mass thickness. Since x depends on the density of the material, this equation is often used in the following form by substituting x with ρt , where t is the thickness of the sample or x-ray path length:

$$\frac{I}{I_0} = \exp \left[-\left(\frac{\mu}{\rho}\right)\rho t \right] \quad (\text{S20})$$

Due to the shallow incident angle of the x-ray (0.6°), its path length t is essentially parallel to the surface of the film. Therefore, we assume only the x-ray passing through the bottom layer (l_0 in Fig. S3) below the top of the silica particles is attenuated by silica particles. We also assume the attenuation effect of the active layers can be neglected compared with that from silica. Since the bottom layer is only partially filled with silica particles with volume fraction, ϕ_{SiO_2} , Eqn. S20 is further modified as:

$$\frac{I}{I_0} = \exp \left[-\left(\frac{\mu}{\rho}\right)_{\text{SiO}_2} \rho_{\text{SiO}_2} t \phi_{\text{SiO}_2} \right] \quad (\text{S21})$$

The value of $\left(\frac{\mu}{\rho}\right)_{\text{SiO}_2}$ is calculated as 36.4 cm g^{-2} for 8 keV x-ray with the data published by Hubbell and Seltzer,³ and ρ_{SiO_2} is 2.32 g cm^{-3} measured by a SANS experiment. Given an estimated ϕ_{SiO_2} of 0.2, we have the attenuation length L_e of 0.59 mm, which is the length to reduce 63 % of the intensity. This value is much smaller than the illuminated length of the sample, which we estimated as approximately 20 mm using a phosphor placed on the sample stage. Therefore, we conclude essentially all the x-ray entering the bottom layer was attenuated, so all the diffracted photons by P3HT crystals came from the top layer (l_1) above the silica particles. In fact, comparing the GIXRD data of samples with or without the silica particles side-by-side, their ratio of intensity is roughly the ratio of l_1 to the total active layer thickness ($l_0 + l_1$). This finding also justifies that only the top region of each sample is measured. However, a quantitative analysis on this system is subjective to many unknown factors, so it is not discussed.

A qualitative analysis of the P3HT (100) peaks shown in Fig. S4 is done with Bragg's law, which gives the d-space of the crystals (d) by:

$$d = \frac{\lambda}{2 \sin \theta} \quad (\text{S22})$$

where λ is 1.54 Å.

Scherrer's relation can also be used to estimate the correlation length of the crystalline domains (L) given as:

$$L = \frac{K\lambda}{\beta \cos \theta} \quad (\text{S23})$$

where K is the shape factor chosen as 0.9 here, and β is the full-width-half-maximum broadening of the peak.

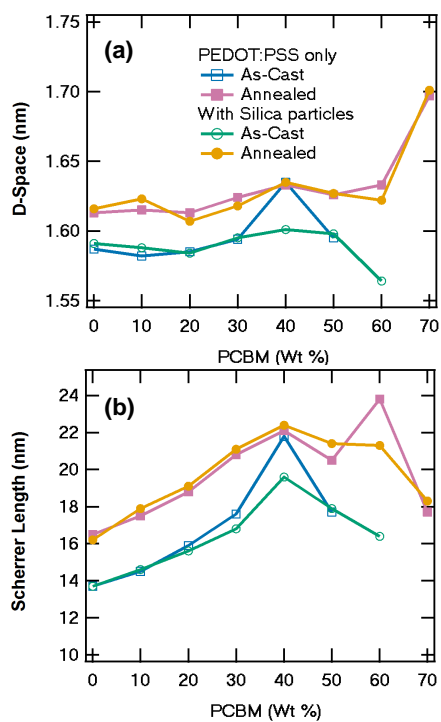


Figure S5 Analysis of GIXRD data using Bragg's law and Scherrer's relation.

By using Eqns. S22 and S23, we calculated the d and L of each data set as shown in Fig. S5. One can clearly see the silica particles have negligible effect on P3HT crystals in the top layer, because the d 's and L 's

between the treatments with or without silica particles are overlapped except for two cases. The first one is the as-cast 40 Wt.% PCBM sample without silica particles. For some unknown reason, the P3HT approached the state of crystallization as if it had been annealed, and the actual annealing afterwards had no further effect. This is also the same data set showing abnormally low SANS intensity in Fig. 4 (a) in the main text. Therefore, there may be something unexpected happened to this sample, but it does not change the conclusions in this report.

Secondly, with silica particles, the samples with 60 Wt.% PCBM shows a higher Scherrer's correlation length after annealing. However, this is the only exceptional data point, which is insufficient to support that the increased correlation length of P3HT is linked to the rearrangement of PCBM. In fact, we also found the general trend of correlation length is counter-intuitive, as one may expect it to decrease with more PCBM.⁴ However, we currently do not have a satisfactory answer to this finding.

Another observations in the GIXRD results also is the increase in the d-space and the correlation length of the P3HT (100) crystals after annealing, which had been explained in the literature.^{5,6} In summary, due to the attenuation effect of the silica particles, no information on the P3HT crystals near the substrate can be obtained by GIXRD. Also, the silica particles have negligible effect on the P3HT crystals near the top of the active layer based on the current results.

References

- [1] M. Teubner and R. Strey, *The Journal of Chemical Physics*, 1987, **87**, 3195–3200.
- [2] J. W. Kiel, B. J. Kirby, C. F. Majkrzak, B. B. Maranville and M. E. Mackay, *Soft Matter*, 2010, **6**, 641–646.
- [3] J. Hubbell and S. Seltzer, *Tables of X-Ray Mass Attenuation Coefficients and Mass Energy-Absorption Coefficients from 1 keV to 20 MeV for Elements Z = 1 to 92 and 48 Additional Substances of Dosimetric Interest*, 1996.
- [4] M.-Y. Chiu, U. S. Jeng, M.-S. Su and K.-H. Wei, *Macromolecules*, 2009, **43**, 428–432.

- [5] B. A. Collins, J. R. Tumbleston and H. Ade, *The Journal of Physical Chemistry Letters*, 2011, **2**, 3135–3145.
- [6] M. A. Brady, G. M. Su and M. L. Chabinyc, *Soft Matter*, 2011, **7**, 11065.